BEAM MEASUREMENTS REQUIRED IN THE FIRST TWO YEARS OF LHC COMMISSIONING

Frank Zimmermann

Abstract

Many beam measurements are essential already in the first stage of the LHC commissioning. Others become necessary only as the intensity and the number of bunches is raised. I will review the beam measurements needed in the various phases of the LHC commissioning, their sequence, and the tools required for performing them. An earlier talk at Chamonix XII has discussed beam measurements on the LHC flat bottom [1]. The present discussion also addresses acceleration and collision, the priority or order of the various measurements, as well as requirements for instruments and timing.

INTRODUCTION

The LHC will be commissioned in stages [2], which are summarized in Table 1. The first stage for protons foresees an initial several-month period with pilot and medium-intensity bunches, followed by 43-bunch operation, which is then extended to 156 bunches. The final pushed parameters of this first stage are characterized by $\beta^* = 2$ m in interaction points (IPs) 1 and 5, a bunch population $N_b = 9\times10^{10}$, and a luminosity of 1.1×10^{32} cm^{-2}s^{-1}. In the second stage of LHC commissioning, 936 bunches are stored per ring with 75-ns separation, avoiding problems with electron cloud, and keeping the number of long-range interactions moderate. The IP beta functions in IPs 1 and 5 are squeezed to 1 m, the bunch population stays at 9×10^{10} protons per bunch, and a crossing angle of about 250 μrad is needed. The luminosity reaches 1.2×10^{33} cm^{-2}s^{-1}. Stage 3 finally refers to 25-ns operation with 2808 bunches, nominal IP beta functions of 0.55 m, about half the nominal bunch intensity, namely $N_b = 5\times10^{10}$, and a luminosity of 1.9×10^{33} cm^{-2}s^{-1}. Now the missing dilution kickers and new 'phase-2' collimators are installed, before the nominal performance and a luminosity of 10^{34} cm^{-2}s^{-1} can be established.

This paper discusses the measurements and instruments needed in the first three stages of LHC commissioning, spanning from the first pilot bunch to 2808 bunches at half the nominal intensity. Measurements, procedures and tools absolutely needed in the first stage are distinguished from those which are either required only in stage 2 or of secondary importance. LHC commissioning sequences with pertinent measurements and instruments were already presented in previous Chamonix workshops, e.g., by M. Lamont [3, 4], H. Schmickler [5, 6], P. Collier [7] and B. Goddard [8]. An updated plan for the various comissioning phases is available on the LHC commissioning web site [9].

ESSENTIAL SYSTEMS

Before at the LHC beams of any significant intensity can be injected, accelerated and collided, three essential components have to be set up: machine protection, beam loss monitors, and collimation.

Machine protection is crucial, since at 7 TeV already a single pilot bunch with an intensity of 5×10^9 protons is close to the damage limit of metallic surfaces, which is estimated at 7×10^9 protons [10, 11]. At injection, the metal damage limit is reached for about 50 nominal bunches [10]. For comparison, the damage limit of the more robust collimators for fast losses is estimated above 3×10^{13} ($\sim$260 nominal bunches) and 5×10^{11} (~ 4 nominal bunches) protons at 450 GeV and 7 TeV, respectively [10]. Fast losses of 10^9 and 5×10^5 protons can lead to magnet quenches at injection and top energy, respectively. The quench limit during a beam dump is reached for about 2×10^6 and 1.4×10^9 protons per meter in the abort gap at 7 TeV and at injection, respectively [12, 13]. For comparison, debunching 43 bunches with $N_b = 9\times10^{10}$ protons each and distributing them around the ring would produce a line density of 1.4×10^8 protons per meter, which is about 100 times higher than the 7-TeV quench limit. Therefore, at 7 TeV losing three percent of the beam from the bucket with 43 bunches, or less than 1 percent with 156 bunches, may result in a critical density at the abort gap. An abort gap monitor will be required, if beam dumps frequently lead to quenches due to this effect.

About 3700 beam-loss monitors (BLMs) are installed in the two LHC rings [14]. They are an integral part of the machine protection system [15]. Calibration of these monitors and their reliability are issues to be addressed early on [16].

The collimation system features about 400 degrees of freedom, which need to be optimized by beam-based adjustments. For example, the collimator jaws must be set to within 50 μrad with respect to the beam direction [17].

At injection the limited mechanical aperture of the cold arc equals 7.2σ [18, 19], accounting for 21% beta beating. The primary collimators are nominally set to 5.7σ [20]. The requirement that the cold-arc aperture should not become the primary aperture of the machine restricts the maximum permissible beta beating to about 90% [1], for

[1] This number needs to be confirmed by the collimation team.

Table 1: Stages of LHC Beam Commissioning [2].

stage	N_b	#bunches	β^*	θ_c	L at IP1 and 5
Ia	$5\times10^9\rightarrow4\times10^{10}$	1	18 m	0	10^{27} cm^{-2}s^{-1}
Ib	$4\times10^{10}\rightarrow9\times10^{10}$	43$\rightarrow$ 156	18 m $\rightarrow$ 2 m	0	$6.8\times10^{29}\rightarrow1.1\times10^{32}$ cm^{-2}s^{-1}
II	$4\times10^{10}\rightarrow9\times10^{10}$	936	18 m $\rightarrow$ 1 m	250 μrad	$1.5\times10^{31}\rightarrow1.2\times10^{33}$ cm^{-2}s^{-1}
III	$4\times10^{10}\rightarrow5\times10^{10}$	2808	18 m $\rightarrow$ 0.55 m	285 μrad	$4.4\times10^{31}\rightarrow1\times10^{34}$ cm^{-2}s^{-1}

low-intensity beams with a single-stage collimation during early commissioning. At higher intensity, with a 2-stage collimation system, the (off-momentum) beta beating should be less than 21% at all times for a maximum closed-orbit error of 4 mm [19].

EXPECTED ERRORS AND TOLERANCES

Table 2 lists data for systematic and random field components in the LHC dipole magnets at injection and their change during snapback. The effect of sextupole spool-piece misalignments, by 0.3 mm on average and 0.6 mm rms, has been taken into account in the values quoted for b_2 and a_2.

Table 2: Table of selected dipole and quadrupole magnet errors, in standard units of 10^{-4} for a reference radius $r_0 = 17$ mm [21]; the values quoted for b_2 and a_2 of the dipoles include the effect of feeddown from systematic and random sextupole spool-piece misalignments of 0.3 mm and 0.6 mm rms, respectively.

multi-	injection		decay	
pole	mean	rms	mean	rms
$\lvert b_1\rvert$	5	6	1.4	1.2
$\lvert b_2\rvert$	($\pm$)1.2	0.6	0.07	0.1
$\lvert a_2\rvert$	0.2	2	0.07	0.3
$\lvert b_3\rvert$	5	2	2	0.5
$\lvert a_3\rvert$	0.1	0.4	0.07	0.07
$\lvert b_2\rvert_{\rm quad}$	—	—	2	2

Momentum

A systematic error in b_1 yields a momentum error of

$$\frac{\Delta p}{p} = \frac{\gamma^2}{\gamma^2-\gamma_{tr}^2}\, b_1 \ . \qquad (1)$$

with $\gamma_{tr}\approx 55.68$ the Lorentz factor for the LHC transition energy. As an illustration, with a b_1 of 10 units, and using $\gamma\approx 479.6$, the momentum error is about 10^{-3}.

Orbit

During the snapback, an rms change of b_1 by 1.2 units, leads to a change in the rms closed orbit of

$$\Delta x \approx \frac{\sqrt{N_{\rm dipole}}\, l_{\rm MB} < \beta >}{\rho}\Delta b_{1,\rm rms}\frac{1}{2\sqrt{2}\sin(\pi Q)} \ , \qquad (2)$$

equal to about 0.7 mm, with $N_{\rm dipole}\approx 1100$ the number of dipoles, and $l_{\rm MB}\approx 14.3$ m the dipole length. During the squeeze an error of 10 units in the D1 dipole can change the closed orbit by 3σ in the triplet quadrupole magnets [22].

Tune

Static tune errors will predominantly arise from errors in the quadrupole gradients or in the dipole field, as well as from (systematic) horizontal orbit offsets in the lattice sextupoles. As a smaller contribution, the systematic misaligment of the sextupole spool-pieces results in a static tune shift of 0.03. Initial total tune errors up to 0.4 may be expected.

Concerning the dynamic variation of the tune, a systematic decay $b_{2,\rm quad}$ by 2 units in the quadrupole strength yields a tune change of about [23]

$$\Delta Q \approx 54|b_2|_{\rm quad}10^{-4} \approx 0.01 \ . \qquad (3)$$

Dynamic tune changes on the ramp also arise from the conspiracy between the snapback of b_3 in the dipoles and the misalignment of sextupole spool-pieces via feeddown. This contribution can be estimated as

$$\Delta Q \approx \frac{1}{4\pi} < \beta > \frac{l_{\rm MB}}{r_0\rho}N_{\rm dipole}\left(\frac{2b_3\Delta_{\rm spool}}{r_0}\right) \ , \qquad (4)$$

where b_3 here refers to the mean decay, and $\Delta_{\rm spool}\approx 0.3$ mm to the systematic error in the spool-piece alignment. From (4) the b_3 decay of 2 units during the snapback yields a tune change of 0.015, while the total change during the ramp is 7/2 times larger, or $\Delta Q\approx 0.05$. Another source of dynamic tune variation are tracking errors between the dipole and quadrupole magnets. The tune change from a relative dipole tracking error $\Delta B_1/B_1$ is

$$\Delta Q \approx Q'_{\rm nat}\frac{\Delta B_1}{B_1} \ , \qquad (5)$$

where $Q'_{\rm nat}\approx 84$ denotes the natural chromaticity of the LHC. The measured magnetic field reproducibility between ramps is $10-50\times10^{-6}$ [24], which implies a tune variation ΔQ of 0.01–0.04. Adding the various contributions, we may expect total dynamic tune changes on the ramp of order 0.1.

Tune shifts during the squeeze are generated by errors in the low-beta quadrupoles: A 10 unit error of a single triplet Q2 magnet changes the tune by 0.03.

Coupling

The static component of coupling at injection is generated by a_2, as well as by quadrupole rolls and orbit offsets in the lattice sextupoles. The three terms contribute about equally, each generating $\kappa_- \approx 0.06$, so that the total coupling can be of order 0.2; see also [25]. The dynamic change in coupling generated by the decaying part of a_2 (including feeddowns) can be estimated from the formula [25]

$$\kappa_- \approx f_- \frac{6}{2\pi} \sqrt{\beta_x \beta_y} \frac{l_{\rm MB} < a_2 >}{r_0 \rho} \, 8 \, , \qquad (6)$$

with $r_0 = 17$ mm, $\rho \approx 2778$ m the bending radius, $l_{\rm MB} \approx 14.3$ m the dipole length, $\sqrt{\beta_x \beta_y} \approx 78$ m, the average beta function in the arc, and the facctor $f_- \approx 15.9$ arising from integrating over all cells of one arc. The factor 6 comes from summing over the 6 magnets of a cell, and the factor of 8 from a pessimistic linear addition of the contributions from all octants. Inserting for $< a_2 >$ the change of 0.07 units (change of effective a_2 including feeddown from the b_3 decay and the systematic misalignment of the sextupole spool pieces) yields $\kappa_- \approx 0.013$ for the variation of the minimum tune distance during the decay and snapback. The change due to the disappearance of the persistent current during the ramp (7 units of b_3) gives a larger coupling change of $\Delta\kappa_- \approx 0.05$. There also is a small contribution to the coupling variation during snapback from an rms orbit change $y_{\rm rms}$ at the sextupoles, which changes the coupling strength by

$$\kappa_- \approx \frac{1}{2\pi} \sqrt{N_{\rm sext}} < \beta > k_s l_{\rm sext} \approx 0.003 \, , \qquad (7)$$

with the sextupole strength $k_s = 0.047$ m^{-3}, sextupole length $l_{\rm sext} = 0.3$ m, and number of sextupoles $N_{\rm sext} \approx 350$.

Beta Beat

The static beta beating at injection or top energy is likely dominated by quadrupole gradient errors and orbit offsets in the lattice sextupoles. The (off-momentum) beta beating expected when all magnet and orbit specifications are met is about equal to the 21% tolerance [26]. However, experience at existing storage rings has typically shown much larger values of beta beating. For example, after the first optics correction, the beta beating in the HERA proton ring was still 400% [27]. For the squeezed LHC optics, a 10 unit error of a single Q2 triplet magnet gives rise to 20% beta beating [22]. The dynamic changes in the beta beating are crucial for collimation and machine protection. The amplitude of the additional beta beating due the change of the random $b_{2,\rm rms}$ can be estimated as

$$\frac{\Delta\beta}{\beta} \approx \frac{\sqrt{N_{\rm dipole}}}{2\sin(2\pi Q)} \frac{< \beta > l_{\rm MB} b_{2,\rm rms}}{r_0 \rho} \, . \qquad (8)$$

Inserting for $b_{2,\rm rms}$ the change by 0.4 units rms, and $N_{\rm dipole} \approx 1100$ the number of dipole magnets, we find a change in the beta beating during the snapback of only 1%. The additional beta beating induced on the ramp by the feeddown from the full b_3 in the dipoles via the spool-piece misalignment will be 7/2 times larger or about 4%. A random rms orbit offset, or change in rms orbit offset, $y_{\rm rms}$, of 1 mm at the lattice sextupoles yields a static or dynamic beta beating

$$\frac{\Delta\beta}{\beta} \approx \frac{\sqrt{N_{\rm sext}}}{2\sin(2\pi Q)} < \beta > l_{\rm sext} k_s y_{\rm rms} \, , \qquad (9)$$

which also amounts to about 1%. The (off-momentum) beta beating expected when all magnet and orbit specifications are met is about equal to the 21% tolerance [26]. However, experience at existing storage rings has typically shown much larger values of beta beating. For example, after the first optics correction, the beta beating in the HERA proton ring was still 400% [27].

Chromaticity

A 1 unit decay of b_3 changes the chromaticity Q' by 45 units. The total decay corresponds to a change in chromaticity $|\Delta Q| \approx 90$, and the change of b_3 during the full ramp by 7 units will result in a (slow) change of chromaticity of $|\Delta Q'| \approx 320$.

2nd Order Chromaticity

Since the measured systematic errors of b_4 and a_3 are much (10 times) smaller than the uncertainties considered in [26, 28], the expected second order chromaticity and its variations during snapback and ramp lie well within the acceptable range. The Landau octupoles and the low-beta squeeze may, however, induce significant second-order chromaticity, of about 20000, which can be corrected by the skew-sextupole families [28, 29].

Error Summary

The estimated static errors at injection, and the dynamic changes during snapback and squeeze are summarized in Table 3.

Table 3: Expected optics errors and their variation for various parts of the LHC cycle during commissioning.

parameter	injection	snapback	ramp & squeeze
orbit	> 20 mm	1 mm	> 5 mm
beta beating	$> 20\%$ (HERA: 400%)	2%	5%
coupling κ_-	0.2	0.013	0.05
tune	0.35	0.025	0.1
Q'	50	90	320
Q''	1000	30	20000
energy	10^{-3}	10^{-4}	10^{-3}

Tolerances

Table 4 compiles tolerances for various optical parameters and compares their magnitude with that of the errors expected in the absence of correction.

Table 4: Expected errors and correction goals for injection, ramp and squeeze [30].

parameter	tolerance	error / tolerance
orbit change	$1\sigma \rightarrow 0.3/0.5\sigma$	~ 6
beta beating	$> 20\%$ (HERA: 400%)	1-40
coupling κ_-	$0.01 \rightarrow 0.001$	20–200
tune change	$0.015 \rightarrow 0.003/0.001$	~ 300
chromaticity Q'	$5 \pm 5 \rightarrow 2 \pm 1$	~ 300
2nd order chr. Q''	1000/2000	~ 10
energy	10^{-4}	10

From Table 4, it is evident that the LHC cannot be commissioned without optics measurements and corrections.

COMMISSIONING STEPS AND PROCEDURES

First Turn and Injection Matching

Necessary steps include (1) threading, closure, and orbit smoothing, (2) the tuning of injection kicker, injection septum, and kicker timing, and (3) the adjustment of the horizontal orbit correctors in each octant to the beam energy from the SPS. Beta matching is considered optional. It could be performed for 43 bunches.

The instruments needed to perform these steps are fast beam-current transformers (BCTs) [31], screens in the injection region showing the beam image on the first passage, as well as the horizontal and vertical readings of the beam-position monitors (BPMs) [32]. Desirable for first-turn steering would also be the sum readings of the BPMs, which could be obtained by using the electronics of the second ring. The BPM sum signal was extremely helpful in the HERA commissioning, where it allowed discriminating valid beam position readings from spurious ones. Alternatively, in the LHC one may get information about beam loss from the auto-triggering of the BPMs. The BPMs can also be used to infer the integer and fractional part of the tune. For the latter, a few turns of circulating beam will be required. The BPM readings should be triggered on the first turn, which is automatically fulfilled, if they are auto-triggered.

RF Capture

The rf phase and rf frequency need to be adjusted to minimize the longitudinal injection oscillation and to center the beam in the aperture, respectively. A measurement of the longitudinal bunch profile and its evolution after injection would be useful for monitoring centroid and bunch length oscillations as well as longitudinal tails. Less importantly, the synchrotron frequency could be measured as a function of rf voltage, which would allow cross-checking the phasing of the rf cavities, the voltage calibration, and the momentum compaction factor.

Required instruments include the arc BPMs (turn-by-turn readings) [32], the fast beam-current transformers (fast BCTs), the dc beam-current transformers (BCTs) [31], and longitudinal profile monitors, e.g., wall-current pick-up signal provided by the rf group.

Extraction & Dump

The extraction and beam dump have to be set up early on, so as not to activate the LHC machine and as a prerequisite for intensities above the pilot bunch. Similar as for injection, the septum and kicker strengths as well as the kicker timing are to be adjusted with the help of screens and BPMs. The local optics in the vicinity of septum and kicker could be checked in order to exclude huge mismatches, which could lead to excessive losses in the extraction channel. The available set of dilution kickers will be turned on and their effect measured shortly after the start of stage I. Dilution kickers are necessary for 156 bunches and likely for 43 to prevent the destruction of the LHC beam dump.

The following instruments will be needed for these commissioning steps: Screens in the extraction region and in front of the beam dump [33], fast BCTs, BLMs at the extraction region and in the dump line, and a post-mortem system recording beam positions and beam losses on the last couple of turns prior to extraction, in particular the turn-by-turn beam position on the last turn.

Orbit Bumps

A versatile technique which can be used for several different types of studies, performed either simultaneously of successively, are orbit bumps. Sliding orbit bumps can identify aperture limitations, magnet misalignments and gross optical errors. Mapping the phyical aperture around the ring likely requires a minimum of 8 bumps per arc and per straight (2 phases, 2 planes and 2 beams) or a total of 128 orbit long bumps for the two rings. If the only goal is to measure the physical aperture, the bumps can be generated by changing the setpoints of the orbit feedback system. If linear optics errors are also to be detected, via the bump leakage [34], it may be advisable to switch of the feedback (in principle the leakage could also be inferred from changes in the feedback corrector currents; however the feedback noise is thought to degrade the quality of such an indirect measurement [35]). The bumps can be used to verify the R_{12} matrix elements of the model or reveal discrepancies. Coupling sources and sextupole fields are detected as orbit changes induced in the plane orthogonal to the bump, and identified by their amplitude dependence.

The orbit bumps may also become a part of the beam-loss-monitor calibration.

The global transverse aperture, physical or dynamical, can be measured either dynamically by kicking the beam so that it fills the entire aperture and detecting the resulting profile, or by exciting two orbit correctors with either sign, one by one, until the beam is lost. For the second approach, the beam can be centered in the available aperture with the two correctors. Assuming the correctors are separated by a betatron phase advance α, not equal to an integer multiple of π, the obstacle limited half aperture a and the equivalent acceptance A are then given by

$$A \equiv \frac{a^2}{\beta_a} = \frac{1}{4}\left(\frac{\sin^{-2}(\pi Q)\theta_1^2\beta_1\theta_2^2\beta_2}{\theta_1^2\beta_1+\theta_2^2\beta_2-2\theta_1\theta_2\sqrt{\beta_1\beta_2}\cos\alpha}\right), \quad (10)$$

where β_a is the beta function at the aperture restriction, $\beta_{1,2}$ denote the beta functions at the location of the two correctors, and $\theta_{1,2}$ the maximum absolute deflection angle, of either sign, that can be applied to the correctors before the beam is completely lost. The expression (10) assumes that there is a single aperture restriction in the ring, as is illustrated in Fig. 1. A particularly simple case is obtained, if the two correctors are 90 degrees apart, or $\alpha = \pi/2$, which roughly corresponds to the phase advance per cell in the LHC arcs.

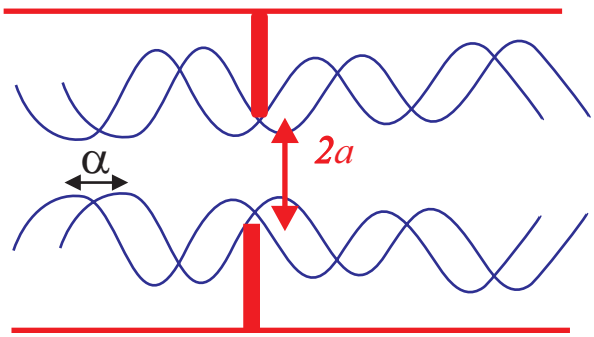

Figure 1: Illustration of global aperture measurement by exciting two orbit correctors, assuming a single aperture restriction.

Instrumentation needed for the bump studies includes BPM readings in orbit mode, beam-loss monitors, and BCTs.

Turn-By-Turn BPM Data

Turn-by-turn beam-position data can be used for determining betatron phase and beta function at the BPM locations. Using the BPM data for both planes, also the local and global coupling is obtained, e.g., via techniques developed at CESR [36], KEKB [37], and RHIC [38]. The turn-by-turn data are expected to yield a clear and reliable image of the LHC optics, since the beam position monitors are densely spaced at every arc quadrupole, with a phase advance of about 45°, which should provide for redundant sampling and, thereby, render the result insensitive to singular faulty BPMs.

In a second stage, together with an rf frequency shift, the turn-by-turn beam position allows detecting off-energy beta beating, sextupole errors, etc. Also data for varying bunch current can be used for measuring and localizing transverse impedance sources.

Obviously, BPM readings in turn-by-turn mode are required for this type of measurement, and, in case of the last item, a fast BCT providing the bunch current.

RF Frequency Scans or Radial Steering

Changing the rf frequency - at CERN called radial steering - allows for a multitude of important measurements, such as ones of dispersion, linear and (less important) nonlinear chromaticity, momentum aperture, and central frequency. Rf frequency shifts may also help when setting up the momentum collimators.

In addition, as mentioned above, in conjunction with turn-by-turn BPM readings, we can obtain the off-momentum beta beating and the off-momentum coupling.

Required for these measurements are BPMs in orbit and turn-by-turn mode, beam-loss monitors, and a BCT.

Detecting Strong Sources of Beta Beat

The fastest way of detecting the beta beat sources is based on a measurement of the betatron phase advance at all BPMs (index i), $\phi_{\mathrm{meas},i}$, and its difference from the model phase advance $\phi_{\mathrm{model},i}$, namely $\Delta\phi \equiv (\phi_{\mathrm{meas},i} - \phi_{\mathrm{model},i})$. Figure 2 illustrates the horizontal beta beating for the two beams which is introduced by a 10^{-3} strength error of the center triplet quadrupole Q2 on the left side of interaction point 1 (the latter is located at position $s = 0$). The beta-beat amplitude is of order 25% and it is slightly larger for beam 2. Figure 3 shows the associated phase beating observed at the BPMs, in a zoomed view covering a length of 1 km downstream of IP 1. The phase beating amplitude corresponding to 25% beta beating is 12–14°. This is much larger than typical phase-measurement errors in the SPS, which are often less than a degree [39] (occasionally SPS phase measurements have shown larger errors of 2–3° [1]), and, therefore, it should be easily detectable also in the LHC.

In general, the quadrupole errors responsible for the measured beta beating (index k), ΔK_k, or, alternatively, the quadrupole-strength changes required for the correction, $-\Delta K_k$, may be obtained from a quasi-inversion of the matrix equation

$$\Delta\vec{\phi} = \mathbf{R}\Delta\vec{K}\,, \quad (11)$$

where $\Delta\vec{\phi}$ denotes the vector of phase differences at N BPMs, $\Delta\vec{K}$ the vector of gradient errors for M

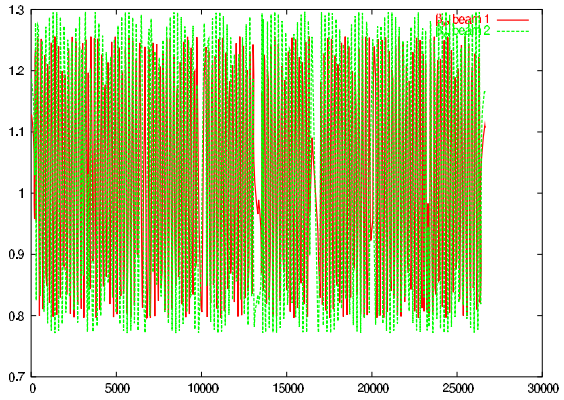

Figure 2: Relative horizontal beta beating $\beta(s)/\beta_0(s)$ generated by a 10^{-3} strength error of Q2 on the left side of IP 1, as a function of position around the LHC ring in units of metre; $\beta_0(s)$ is the design beta function at position s.

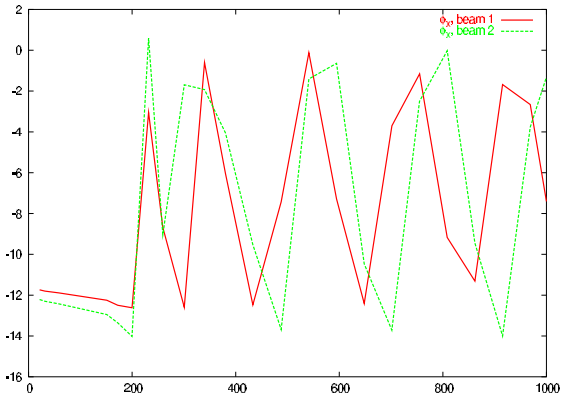

Figure 3: Phase beating in degrees at the BPMs as a function of position in metre over the first 1 km of the LHC ring; the beating was generated by a strength error of 10^{-3} for Q2 on the left side of IP 1.

quadrupoles, and the response matrix R contains the elements [39]

$$\Delta\phi_i = \begin{cases} \left[\frac{\beta_k \cos(\phi(i)-2\phi_k+2\pi Q_0)\sin\phi(s)}{2\sin(2\pi Q_0)}\right]\Delta K \\ \text{for } \phi_{\rm i} < \phi_{\rm k}\ , \\ \left[\frac{\beta_k}{2} - \frac{\beta_k \cos(\phi_i-2\phi_k)\sin(\phi(s)-2\pi Q_0)}{2\sin(2\pi Q_0)}\right]\Delta K \\ \text{for } \phi_{\rm i} > \phi_{\rm k} \end{cases} . \tag{12}$$

where Q_0 is the tune without the quadrupole errors. In the case of the LHC, the matrix R could be the combined response matrix for the two rings, including phases at common BPMs and errors of shared quadrupoles. The availability of data from two beams should facilitate the proper identification of gradient errors in the high-beta regions around the primary collision points.

Gradient errors may also be obtained by global multi-parameter fits of orbit response data in LOCO style [40, 41], where the orbit response to all ring correctors is measured one by one. This is likely much more time consuming than taking turn-by-turn data. A faster variant would consist of exciting only 3 pairs of correctors per plane, again followed by an appropriate fit. The latter technique is applied in KEKB [42]. A possible advantage is the 10-times higher resolution of the BPM orbit reading compared with the turn-by-turn measurement.

For either method, a fit to an optics model is necessary. Application software and an online model could greatly speed up the beta-beat measurement and its correction.

The localization of beta beating sources requires BPMs in either turn or orbit mode.

Ramp

On the ramp we will encounter many dynamic changes: the initial rapid snapback (regeneration of persistent currents), power-converter tracking errors between quadrupoles and dipoles, and the gradual reduction of the persistent current as the magnet current is increased all conspire to render operation interesting. Fast significant tune changes are expected. Therefore, a quasi-continuous tune signal, as soon as possible augmented by a tune feedback, is recommended. Frequent chromaticity measurements during the ramp may also be necessary, either using the conventional radial steering, or a fast rf phase modulation together with a phase-locked loop for the tune measurement [43], or a head-tail monitor plus kick excitation. Chromaticity measurements on the RHIC ramp have been performed by a PLL tune meter in combination with radial steering [44]. The chromaticity evolution in the first seconds of the Tevatron ramp, during the snap back, has been measured by a headtail monitor [45]. However, if the LHC chromaticity if sufficiently reproducible, one might measure and correct it also by changing the rf frequency for successive ramps (classical Tevatron approach) or it can be measured and corrected once at the start of a run (classical RHIC approach). Another back-up solution could be a coherence monitor, as is also employed in RHIC [46]. This monitor is described in the appendix.

Beta beating and coupling need also to be controlled on the ramp. Presumably at higher energy the pertinent tolerance on the beta beating could be relaxed, since the relative arc aperture widens, until the collimators are closed for the squeeze. The coupling must remain corrected at a level which permits tune control.

Needed instrumentation for the ramp comprises the baseband Q (BBQ) meter, augmented by a phase-locked loop (PLL) for tune control, radial steering for chromaticity measurements (RHIC, HERA), the headtail chromaticity monitor, and turn-by-turn BPM readings. Synchronization at the level of 10s of turns is required between various types of equipment. For example, one will want to kick the beam on the ramp and measure the resulting oscillations with the turn-by-turn BPM mode. Acquiring also the tune and the chromaticity at the same instant would be an ad-

vantage, and provide a full optics snapshot at a particular time of the ramp.

Instruments which could come at a later stage are a 'tickler' for weakly exciting individual bunches, e.g., for tune measurements or optics control, and a Schottky tune monitor.

Squeeze

For the squeeze, we can either apply the same techniques as for the ramp, and/or we can proceed in steps with static corrections at the stops. In Chamonix XIV, the correction with stops was not thought to be meaningful for the ramp. However, in case of the squeeze persistent-current effects in the triplets are considered too small to cause complications.

At a later time, e.g., for the commissioning phase II, a special triplet alignment optics [47] is available which can be used to define a reference straight line for the triplet alignment. This will aid in disentangling strength errors of the D1 and D2 separation dipoles from misalignments of the triplet [48]. It seems preferred to perform the triplet alignment at injection energy.

Diagnostics and tools needed to commission and control the squeeze are the BBQ tune monitor, ideally with phase-locked loop, radial steering (as in RHIC, HERA), head-tail chromaticity monitor, turn-by-turn BPM readings, synchronization of beam kicks with BPM readings, tune and chromaticity measurements, and, later, a Schottky monitor.

Beam Evolution and Lifetime

Monitoring the dc beam current and the bunched beam curent as a function of time yields the dc beam lifetime and the bunch lifetime. At 7 TeV particles which leave the rf bucket are lost after about 6.5 minutes due to synchrotron radiation (at injection after 390 hours) [49]. We will also want to measure the beam size and bunch length evolution during a store, as well as monitor the bunch structure and density inside the abort gap. From stage II onwards, we will also be interested in detecting beam tails and performing measurements of diffusion rates.

The suite of instruments required includes BCT, fast BCT, bunch length monitor (e.g., wall-current monitor provided by the rf group), wire scanner, synchrotron-light monitor and/or ionization profile monitor for the transverse beam size [50]. For stage II, we wish the Schottky monitor, a fast scraper (for diffusion measurements), the abort gap monitor, and a tail monitor.

With its nominal speed the wire scanner should be able to scan up to two complete PS batches in the LHC at 7 TeV [50]. The initial wire scanner will have a reduced speed, so that it can only be used for a few bunches. The main use of the wire scanner may be the calibration of the other two transverse profile monitors, which are based on synchrotron radiation and gas ionization, respectively, and are both capable of sustaining the full LHC beam intensity.

Collision and Luminosity

To bring the two LHC beams into collision, a 2-dimensional transverse scan and a longitudinal scan of the beam position or rf phase, respectively, are necessary. Later on, with nonzero crossing angle, the transverse and longitudinal collision points are coupled. Since a good equalization of the transverse beam sizes is important, it will be advantageous to have in hands IP tuning knobs, for equalizing the IP beta functions or correcting IP coupling and dispersion. The detection and control of a spurious crossing angle may also prove important. The TOTEM experiment requires a knowledge of the crossing angle with a precision of 0.2μrad, to be compared with an expected resolution from the interaction-region BPMs of $\Delta\theta_c \approx 10\ \mu$m [51], without taking into account any possible degradation of the BPM signals by collision debris. Considering a BPM resolution of $5\ \mu$m at a distance of $\sim$20 m at either side from the IP, one might think that the crossing angle could be measured with a resolution of the order $2 \times 5 \times 10^{-6}/20 \approx 0.5\ \mu$rad. However, the crossing-angle resolution is limited by the systematic error in the zero BPM reading for the two beams (taken from the two sides of the monitor stripline using different electronics), which is of order 200 μm [52].

The measurement and control of the crossing angle to within 10μrad precision is consistent with the operational experience at the Tevatron [53]. At the Tevatron crossing angles of 20–40 μrad increase detector backgrounds by 40%, which is attributed to the detector geometry [53]. By contrast, at RHIC the crossing angle is kept constant only at the level ± 0.5 mrad (twice the nominal LHC crossing angle) due to unreliable BPMs at the separation dipoles and due to diurnal orbit motion caused most likely by thermal movement of the triplet quadrupoles [54]. The RHIC proton stores show a poor reproducibility and lifetime problems, which could be related to the lack of crossing-angle control [54].

Instrumentation required includes the beam-position monitors in the interaction region [32], in particular the stripline BPMs which are common to both beams, and a luminosity monitor. A 'granular' luminosity was expected to potentially fulfil the TOTEM requirements [51], but no such monitor is foreseen at the LHC.

Collective Effects

Already in LHC stage I, we may encounter a number of collective effects, since the bunch intensity reaches 9×10^{10}, which is 80% of the nominal value. A controlled blow up of the longitudinal emittance will both reduce emittance growth rates from intrabeam scattering and also suppress beam instabilities.

The reduction of intrabeam scattering is easily estimated. Assuming half the nominal longitudinal emittance (namely 1.25 eVs), the longitudinal emittance growth rate due to intrabeam scaterring is about 24 h, and the horizontal one 86 h, scaling the numbers of [55]. The controlled blow up of the longitudinal emittance to its nominal value of 2.5 eVs,

as planned for the nominal scheme, increases the emittance lifetime to 75 h longitudinally, and 134 h horizontally.

The effect of the crossing angle on the luminosity can be studied during stage I, in order to derive tolerances and to prepare stage II.

Measurements of the betatron tune as a function of single-bunch current with collimators open and closed can be performed at injection, in order to validate impedance estimates, which will be important in view of the subsequent intensity raises in stages II and III.

During these latter two stages, additional experiments become possible and necessary, such as a study of the effect of the long-range beam-beam collisions, and watching out for signs of the electron cloud, e.g., electron flux at the wall, pressure rises, heat load on the cryogenic system, tune shift along a bunch train, incoherent tune spread, single- and coupled-bunch instabilities.

To observe and control these collective phenomena we again require interaction-region BPMs, in particular the common stripline BPMs, and luminosity monitors. Later, for stages II and III, bunch-by-bunch and turn-by-turn BPMs, electron-cloud diagnostics [56], synchrotron-light monitor, ionization profile monitor, and Schottky detectors will also be desired.

Schedule of Instrumentation Needs

The instruments and their required functionality for the various stages of LHC commissioning, according to the discussion in this chapter, are summarized in Fig. 4.

SUGGESTIONS

'Sacrificial' Non-Colliding Bunches

Sacrificial non-colliding bunches are used at several colliding-beam storage rings, for example at HERA [57] and KEKB [42]. Such non-colliding bunches can be employed for precise diagnostics and control, e.g., for measuring and controlling the tunes, the beta functions, dispersion, dynamic aperture, without any degradation due to the collision, whereas non-colliding bunches suffer from beam-beam tune spread, coherent beam-beam modes, and poor lifetime in case of mismatched beam sizes (for example, after an optics diagnostics kick, or a head-tail chromaticity measurement), all of which complicate diagnostics and feedback.

At KEKB, a clear tune signal can only be measured for the non-colliding bunches, and it is this signal which is used by the tune feedback [42]. The current-dependent feedback setpoints take into account the tune differences between the non-colliding test bunches and the majority of colliding bunches.

Non-colliding bunches in LHC could be excited by a fast tune kicker, a gated aperture kicker, or a bunch-selective 'tickler' derived from the transverse damper.

Further benefits include the measurements of emittance growth and beam lifetime for a non-colliding bunch, which can be compared with those of colliding bunches under otherwise identical conditions. Thereby, beam-beam effects can be unambiguously separated from other phenomena like IBS or gas scattering.

At HERA the non-colliding bunches are greatly valued by the experimenters, since they allow a continual recording of beam-gas experimental backgrounds [57]. A similar proposal for measuring single-beam rates in the LHC experiments has been made by K. Potter [51, 58], who suggested to shift the rf phase slightly for the two beams, to leave some bunches without counterpart. The scheme of non-colliding test bunches could serve the same purpose.

Monitors and Procedures Useful at Other Colliders

Experience at other colliders suggests a number of useful tools and instruments.

The BPM sum signal was instrumental for steering the first turn in HERA, since it allowed discriminating between reliable and spurious BPM readings.

Fits to online optics models were a standard means in the control system of the SLC and PEP-II. Typically, here a region of an accelerator could, or can, be selected for a fit to the model, and the fit then extrapolated over a larger range. Deviations between extrapolated model and measurement help identifying regions with optics errors. The user can select between different underlying models (typically TRANSPORT, DIMAD, MAD,...) in various refinements, and the fit and display are available in real time within seconds, while, for example, a magnet strength is being varied.

Application software for all instruments will be helpful. During HERA commissioning, at times only specialist software was available, which slowed down the progress.

History buffers at SLC and PEP-II allowed, or allow, post-analysis and cross correlations between any measured beam property (orbit, intensity, tune, beam size,...), magnet settings, outside temperature, etc. The data stored intially at 120 Hz or 10 Hz are sparsified after about one month. The sparsified data sets are available for all years since the start of the SLC. This gives ample opportunity to track and to understand changes in the accelerator performance. The control system also offers correlation functions and histograms for displaying the data.

At RHIC and HERA, Schottky tune monitors were highly appreciated.

The coherence monitor at RHIC was already mentioned. It is described in the appendix.

The electronic logbook at the Tevatron is valuable and well structured. Every person on the FNAL site can add comments or subsequent analyses. Any pictures taken on scopes or screens can be added with the click of a mouse. The logbook can be read from the office, and it offers a comprehensive and up-to-date overview of the achievements during the previous shift or day.

Wide-band wall current monitors are in use at HERA and

	Stage Ia	Stage Ib	Stage II	Stage III
BPMs	orbit, turn-by-turn for 1 bunch, BPM sum		position bunch-by-bunch and turn-by-turn	
BLMs				
BCTs, fast BCTs	bunch-by-bunch current			
wire scanners	on user request, only few bunches		timing synchronization, higher speed with up to 2 PS batches at 7 TeV	
screens	1st turn	+β matching if necessary	injection matching monitors	
abort gap monitor				
longitudinal profile	wall current monitor			
synchrotron light	average beam size		bunch-by-bunch beam size	
IPM	average beam size			
BBQ	average tune		tune of selected bunch	
Q', coupling	radial steering, HT, BBQ-PLL, BBQ-HT, average chromaticity			
luminosity	average luminosity		bunch-by-bunch luminosity	
e-cloud			e- diagnostics	

Figure 4: Instrumentation schedule including functionality cuts proposed by the BDI group for LHC commssioning stages Ia and Ib (see Table 1). Shown in dark blue are equipments and measurements considered essential for stage I. Indicated by green-blue color are tools which are either of secondary importance or whose commssioning could be delayed.

at the Tevatron for monitoring the longitudinal bunch profile and its evolution, including centroid oscillations due to injection errors, quadrupole oscillations, or tail growth. At HERA this monitor was used for phase and enery adjustements at injection.

Equally at HERA, an ionization profile monitor was in continual operation. It delivered information of the transverse beam profiles and the emittances. A measurement of the dynamic aperture using the ionization profile monitor is illustrated in Fig. 5. Here, the beam was intentionally injected with an offset, so that the entire aperture was filled. The lifetime of the stored beam was poor, evidenced by the decay in the beam profile over 1 minute. The amplitude beyond which no beam particles are observed corresponds to the short term dynamic or physical aperture. Using the measured beta function at the monitor, the dynamic acceptance for this example was $A_{\rm dyn} \approx 1.2$ μm [59], significantly smaller than the linear acceptance $A_{\rm lin} \approx 2.3$ μm, which was measured in a static way by exciting pairs of orbit correctors until the beam was fully lost, applying Eq. (10).

Also at HERA, a beam-beam coupling monitor was used for bringing the two beams into collision.

BEAM-BEAM COUPLING MONITOR

The HERA coupling-monitor was constructed by S. Herb [57, 60], following a method invented by A. Piwinski for the DORIS-I double-ring collider [61]. A similar scheme was also developed by J.-P. Koutchouk for the CERN ISR [62].

A schematic of the HERA apparatus is displayed in Fig. 6. The device consists of the following elements: The electron beam is excited using its tune PLL. The response of the proton beam at the electron-tune frequency is detected. The transverse position of one beam is scanned in two dimensions.

Figures 7 presents typical results from a vertical scan with horizontal excitation, while Fig. 8 shows a horizontal scan. When the scan is performed in the plane of excitation characteristic side maxima are observed. These and the central peak correspond to extrema in the first derivative of the beam-beam deflection force with respect to the

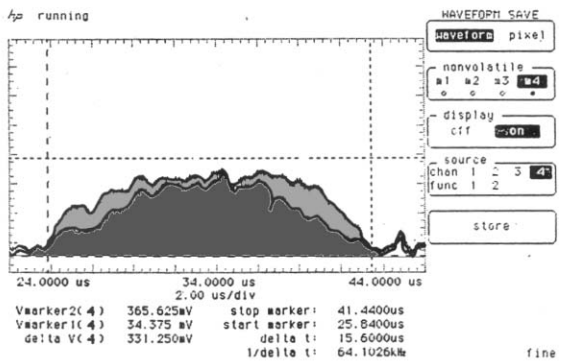

Figure 5: Dynamic aperture measured with an ionization profile monitor in the HERA proton ring. Shown is the horizontal beam profile recorded directly after poor injection with a large offset and beam loss, which filled the available — dynamic or physical — aperture, (upper trace) and 1 minute later (lower trace) [59].

plane of excitation.

For beam-beam separations close to the secondary maxima, an extremely poor beam lifetime was observed at HERA. This is attributed to the strong nonlinearity of the beam-beam force near this point.

The beam-beam coupling monitor offers several advantages compared with scans using luminosity measurements [57]: (1) the beam excitation coupling is completely independent of the luminosity measurement and almost background free, which could be a decisive plus, especially for the pilot bunch intensities, where the LHC luminosity monitor may be blind [63]; (2) its fastness and sensitivity suggest an automation; (3) two one-dimensional scans are sufficient to bring the beams into collision due to the long-range nature of the beam-beam effect. If there are multiple interaction points, a complication arises. In this case, the detected signal is the vector sum of the individual beam-beam kicks, dependent on the different phase advances of the two beams between the collision points, unless the beams are separated at all but one IP at a time.

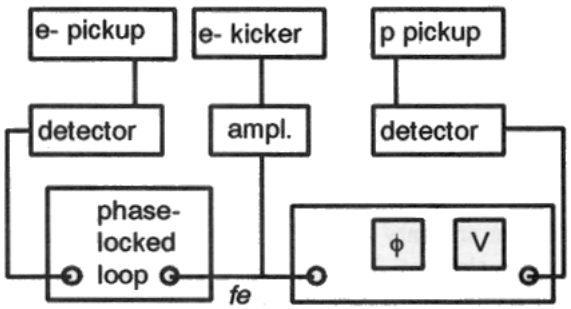

Figure 6: Simplified schematic of the beam-beam coupling monitor apparatus at HERA [60].

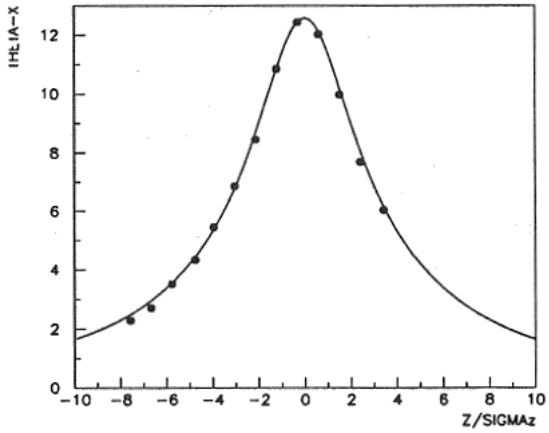

Figure 7: Measured beam-beam coupling signal strength for a vertical scan; the points are measured data, the curve is the theoretical curve derived for a Gaussian beam with an aspect ratio of 3.7:1 [60].

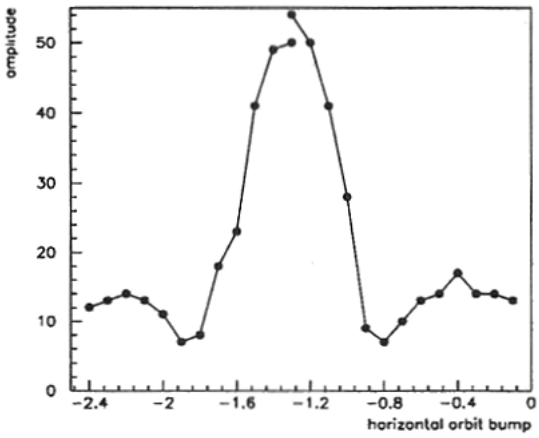

Figure 8: Beam-beam coupling signal measured during a horizontal scan; the horizontal scale is arbitrary; the solid line connects the measured points [60].

CONCLUDING REMARKS

Experience at LEP, Tevatron, RHIC and many other colliders suggests that redundant diagnostics will be helpful fir the initial stages of the LHC. The instrumentation speeds up the commissioning and understanding, and it is especially important at the start of a new accelerator. The diagnostics and measurements help in preparing the subsequent stages and they allow for an early detection of problems ahead.

As an anecdotical example, illustrating the potential merit of preparative measurements, the HERA electron ring was initially commissioned in dedicated runs two or three years before the proton ring. These pre-runs were performed only at low beam current, i.e., below 0.3 mA. Had one raised the electron current to 3–10 mA (its design value

is 58 mA), one would have encountered the threshold of a severe beam lifetime breakdown later ascribed to trapped dust particles. In the absence of such studies, no precaution or countermeasures were taken, and the lifetime problem was discovered only during the final two-beam commissioning of HERA [64, 65]. It hampered HERA operation for a number of years, ultimately necessating a complete replacement of the distributed ion pumps in the dipole vacuum chambers all around the electron ring. Indeed, the dust trapping in the electron was the most severe problem faced during the HERA commissioning, while the anticipated problems like persistent current, proton-ring dynamic aperture, asymmetric beam-beam interaction, etc., all proved fairly benign.

Similarly, while much of the world had expected that B factory performance would be limited by fast beam-ion instabilities in the electron rings, these ion instabilties turned out to be easily suppressed by the multibunch feedback systems in both PEP-II and KEKB. The real limitation for either factory instead proved to be the single-bunch electron-cloud instability in the positron rings, which was discovered and understood only during the KEKB commissioning, and which occurred in PEP-II despite of the fact that after applying TiN coating to the arc vacuum chambers no electron-cloud build up had been expected.

These two examples suggest that we better not rule out the encounter during commissioning of 'unknown unknowns' [66] whose proper understanding will likely require reliable and comprehensive beam diagnostics.

ACKNOWLEDGEMENTS

I thank Ralph Aßmann, Gianluigi Arduini, Roger Bailey, Luca Bottura, Hans Braun, Oliver Brüning, Helmut Burkhardt, Stephane Fartoukh, Wolfram Fischer, Marek Gasior, Massimo Giovannozzi, Brennan Goddard, Jean-Jacques Gras, Bernard Jeanneret, Alex Koschik, Jean-Pierre Koutchouk, Robert Michnoff, Hitoshi Murayama, Francesco Ruggiero, Stephane Sanfilippo, Hermann Schmickler, Rüdiger Schmidt, Tanaji Sen, Ralph Steinhagen and many other colleagues for helpful discussions and information.

APPENDIX - RHIC COHERENCE MONITOR

The RHIC coherence monitor measures the rms value of the beam oscillations in real time. The monitor has been described by R. Michnoff and W. Fischer as follows. A beam position monitor pickup provides the inut to an analog signal conditoning module, which normalizes the difference signal to the sum, and computes the rms of the normalized difference signal using an Analog Devices AD8361. The rms output is digitized and logged at 720 Hz during a RHIC ramp. The measured coherence signal approximately indicates the amplitude of the beam oscillations. One difficulty with the measurement is that due to filtering the measured signal depends on the duration of the beam oscillations as well as on its amplitude. For example, a very short duration high-amplitude coherence signal may produce results similar to a longer duration low-amplitude one. In any case, the RHIC chromaticity on the ramp is fine adjusted by hand when a signal has been observed on the coherence monitor.

REFERENCES

[1] F. Zimmermann, "Flat Bottom Optimization and Tuning," Proc. Chamonix XII, LHC Performance Workshop Chamonix, p. 242 (2003).

[2] R. Bailey, "Summary of Overall Commissioning Strategy for Protons," Session 1 - The Minimum Workable LHC – Plans and Requirements for Beam Commissioning, Years 1 and 2, Chamonix XV Workshop, Divonne (2006).

[3] M. Lamont, "Commissioning with Beam: Overall Strategy," LHC Project Workshop, Chamonix XIV, CERN (2005).

[4] M. Lamont, "Commissioning with Beam: Session Summary," LHC Project Workshop, Chamonix XIV, CERN (2005).

[5] H. Schmickler, "Running In the Diagnostics," LHC Project Workshop, Chamonix XIII, Chamonix (2004)

[6] H. Schmickler, "Beam Commissionng of Instrumentation," LHC Project Workshop, Chamonix XIV, CERN (2005)

[7] P. Collier, "450 GeV," LHC Project Workshop, Chamonix XIV, CERN (2005)

[8] B. Goddard, "Commissioning with Beam of the LHC Transfer Lines and Injection Systems," LHC Project Workshop, Chamonix XIV, CERN (2005).

[9] *http://lhccommissioning.web.cern.ch/*

[10] B. Jeanneret, H. Burkhardt, "Functional Specification: On the Measurement of the Beam Losses in the LHC Rings," LHC-B-ES-0001 Rev 2.0 (2004).

[11] J.B. Jeanneret, D. Leroy, L. Oberli, T. Trenkler, "Quench Levels and Transient Beam Losses in LHC Magnets," LHC-Project-Report-044 (1996).

[12] B. Goddard and B. Jeanneret, "Critical Beam Density in the Abort Gap and Longitudinal Profile Monitor," LHC Commissioning Committee, 17 July 2002 (2002).

[13] C. Fischer, "Functional Specification: High Senstivity Measurement of the Longitudinal Distribution of the LHC Beams," LHC-B-ES-0005.00 rev 2.0 (2003).

[14] R. Jones, "Beam Instrumentation Status," LHC MAC no. 18, 08. December 2005 (2005)

[15] R. Schmidt, J. Wenninger, "Machine Protect Issues and Strategies for the LHC," LHC Project Report 784 (2004).

[16] B. Dehning, "Commissioning of Beam Loss Monitors," Session 1 - The Minimum Workable LHC — Machine Protection and Collimation, Chamonix XV Workshop, Divonne (2006).

[17] R. Assmann, J.B. Jeanneret, D. Kaltchev, "Efficiency for the Imperfect LHC Collimation System," EPAC 2002, Paris (2002).

[18] J.B. Jeanneret, R. Ostijic, "Geometrical Acceptance in LHC Version 5.0," LHC Project Note 111 (1997).

[19] S. Redaelli, R. Assmann, G. Robert-Demolaize, "LHC Aperture and Commissioning of the Collimation System," LHC Project Report Chamonix XIV (2005).

[20] R.W. Aßmann, private communication (2005).

[21] S. Sanfilippo, private communication (2006).

[22] O. Brüning, "Squeeze Criteria & Requirements," LHC Project Workshop Chamonix XIV (2005).

[23] O. Brüning, "Accumulation and Ramping in the LHC," Chamonix X, p. 198.

[24] V. Granata et al., "Magnetic Field Tracking Experiments for LHC," LHC Project Report 738 (2004).

[25] O. Brüning, "Linear Coupling Compensation for the LHC Version 6.1," EPAC 2000, Vienna (2000).

[26] S. Fartoukh, O. Brüning, "Field Quality Specification for the LHC Main Dipole Magnets," LHC Report 501 (2001).

[27] R. Bacher et al., "First Commissioning of the HERA Proton Ring – A Summary of the HERA Proton Run 1," compiled by W. Schuütte and F. Willeke, Harz Seminar, Bad Lauterberg, DESY HERA 92-07 (1992)

[28] S. Fartoukh, J.-P. Koutchouk, "Functional Specification: On the Measurement of the Tunes, Coupling and Detunings with Momentum and Amplitude in LHC," LHC-B-ES-0009 rev 1.0 (2004).

[29] S. Fartoukh, "Second Order Chromaticity Correction of LHC V6.0 at Collision," LHC Project Report 308 (1999).

[30] S. Fartoukh, private communication and discussion (2006).

[31] C. Fischer, R. Schmidt, "Functional Specification: On the Measurements of the Beam Current, Lifetime and Decay Rate in the LHC Rings," LHC-BCT-ES-0001 rev 1.0 (2005).

[32] J.-P. Koutchouk, "Functional Specification: Measurement of the Beam Position in the LHC Main Rings," LHC-BPM-ES-0004 rev 2.0 (2002).

[33] J. Wenninger, B. Goddard, "Functional Specification: Instrumentation for the LHC Beam Dumping System," LHC-B-ES-0008 rev 2.0 (2004).

[34] S. Kamada, "Experimental Techniques and Observations of Nonlinear Dynamics in Particle Accelerators," Workshop on Nonlinear Dynamics in Particle Accelerators, Theory & Experiment, Arcidosso, Italy, AIP Conf. Proc. 344, 1–10 (1994).

[35] R. Steinhagen, private communication (2006).

[36] D. Sagan and D. Rubin, "Linear Analysis of Coupled Lattices," PRST-AB 2, 074001 (1999).

[37] E. Perevedentsev, "Measurement of X-Y Coupling Parameters," KEKB, unpublished note, April 4, 2000.

[38] W. Fischer, "Robust Linear Coupling Correction with N-Turn Maps," PRST-AB 6, 062801 (2003).

[39] G. Arduini. C. Carli, F. Zimmermann, "Localizing Impedance Sources from Betatron Phase Beating in the CERN SPS," Proc. EPAC 2004, Lucerne (2004).

[40] J. Safranek, "Experimental Determination of Storage Ring Optics Using Orbit Response Measurements," NIM A388, 27 (1997).

[41] J. Wenninger, "Orbit Response Measurements at the SPS," CERN-AB-2004-009 (2004).

[42] K. Akai et al., "Commissioning of KEKB," NIM A499, 191 (2003).

[43] O.S. Brüning et al., "Chromaticity Measurements via RF Phase Modulation and Continuous Tune Tracking," EPAC'02 Paris, CERN-SL-2002-037 (2002).

[44] S. Tepikian et al., "Measuring Chromaticity along the Ramp using the PLL Tune-Meter in RHIC," EPAC 2002, Paris (2002).

[45] V.H. Ranjibar et al., "Commissioning of the HEead-Tail Monitoring Application for the Tevatron," EPAC'2004 Lucerne (2004).

[46] R. Michnoff, W. Fischer, private communication, 12.01.2006.

[47] A. Verdier, "Alignment Optics for LHC," LHC-PROJECT-NOTE-325 (2003).

[48] O. Bruning, "Squeeze Criteria & Requirements," LHC Project Workshop, Chamonix XIV, CERN (2005).

[49] F. Zimmerman and M.-P. Zorzano, "Touschek Scattering in HERA and LHC," LHC Project Report 244 (2000).

[50] C. Fischer, "Functional Specification: Measurement of the Transverse Beam Distribution in the LHC Rings," LHC-B-ES-0006 rev 1.0 (2003).

[51] R. Assmann, J.-P. Koutchouk, M. Placidi, E. Tsesmelis, "Functional Specification: On the Measurement of the Relative Luminsoity in LHC," LHC-B-ES-0007 rev 1.1 (2004).

[52] R. Jones, private communication at the Divonne workshop (2006).

[53] V. Shiltsev, private communication, 29.08.2005.

[54] W. Fischer, private communication, 29.08.2005.

[55] F. Zimmermann, "Intrabeam Scattering with Non-Ultrarelativistic Corrections and Vertical Dispersion for MAD-X," CERN-AB-2006-002 (2006).

[56] J.M. Jimenez, "Engineering Change Order - Class 1: Electron Cloud Diagnostics in the LHC," LHC-VI-EC-0001 (2003).

[57] F. Zimmermann et al., "Beam Finding Allgorithms in HERA," Proc. B Factories: The Stae of the Art in Accelerators, Detectors, and Physics, Stanford, California, April 6–10, 1992, and DESY HERA 92-10 (1992).

[58] K. Potter in 1st Luminosity Workshop, 9/12/2002, *http://est-div-lea.web.cern.ch/est-div-lea/luminosity/1st_lumi_workshop.htm*

[59] F. Zimmermann, "Dynamische Apertur und Emittanzwachstum im HERA-Protonen-Ring," HERA Seminar, Bad Lauterberg, Harz, 1993, p. 139 (1993).

[60] S. Herb and F. Zimmermann, "Measurement by Tune Coupling of the Overlap of Colliding Bunches in HERA," Proc. HEACC'92, Hamburg, p. 227 (1992).

[61] A. Piwinski, "Einstellung der Kreuzung der beiden Strahlen mit Hilfe des Raumladungseffektes," DESY H2-75/03 (1975).

[62] J.-Y. Hemery, A. Hofmann, J.-P. Koutchouk, S. Myers, L. Vos, "Investigation of the Coherent Beam-Beam Effects in the ISR," PAC 81, Washington DC, IEEE Trans. Nucl. Sci. 28, 2497–2499, and CERN-ISR-OP-CO-TH-RF-81-13 (1981).

[63] E. Bravin, “Bringing the First LHC Beams into Collision at all 4 IP’s,” Session 5 - Experiment-Machine Interface, Chamonix XV Workshop, Divonne (2006).

[64] F. Zimmermann, “Trapped Dust in HERA and DORIS,” DESY-HERA-93-8 (1993).

[65] F. Zimmermann, J.T. Seeman, M. Zolotorev, W. Stoeffl, “Trapped Macrparticles in Electron Storage Rings,” PAC’95 Dallas (1995).

[66] D. Rumsfeld, US Department of Defense News Briefing 12.02.2002; quoted by H. Murayama at Nanobeam’05, Kyoto, October 17–21 (2005).